

## Supporting information: A paper based, all organic, reference-electrode-free ion sensing platform

Johannes Kofler<sup>a</sup>, Sebastian Nau<sup>a</sup> and Emil J. W. List-Kratochvil<sup>a,b</sup>,

### S1 Numerical calculations

There are well established theoretical models which describe ISM under equilibrium conditions and there are also analytical as well as numerical models for chronopotentiometric operation modes.<sup>1-6</sup> Within these models, the potential at the interface is calculated by inserting the boundary concentrations of the relevant ions in the respective phase into the Nernst equations and the mass transport through the interfaces is described by constant heterogeneous rate constants. The ratio of the heterogeneous rate constants of a specific ion are assumed to be equal to the partitioning coefficient. Hence, these models assume that the thermodynamically facilitated IT is fast and instantaneously, reaching local thermodynamic equilibrium across the interface even under dynamic mass transport conditions. Though, the equilibrium assumption is usually completely justified, they neglect the influence of the electric potential on the transfer rates. For that reason, numerical calculations which take into account the standard ion transfer potential (standard Gibbs free energy of transfer) of all ions involved, at the back and front side of the ISM, were carried out.

Here, we aim to model the membrane using the free energies of transfers and electric field dependent transfer rates at the ISM-liquid interface. Similar to the method described in ref. <sup>7</sup> and ref. <sup>2</sup> the system was separated into three separate layers (analyte, ISM, inner filling solution) (see figure S1). The bulk of these layers were calculated by solving the Nernst Planck and Poisson differential equations (NPP) as described in ref. <sup>2</sup> in the following form:

$$\frac{\partial c_i(x, t)}{\partial t} = \frac{\partial J_i(x, t)}{\partial x}$$
$$\frac{\partial E(x, t)}{\partial t} = \frac{1}{\varepsilon_{o/w}} I(t) - \frac{F}{\varepsilon_{o/w}} \sum_{i=1}^r c_i J_i(x, t)$$
$$J_i(x, t) = -D_i^{o/w} \frac{\partial c_i(x, t)}{\partial x} + \frac{F}{RT} D_i^{o/w} z_i \cdot c_i(x, t) \cdot E_i(x, t)$$

Where  $E$  is the electric field,  $\varepsilon_{o/w}$  is the dielectric constant in the organic/water phase,  $c_i$  is the concentration of the  $i^{\text{th}}$  ion,  $J_i$  is the flux,  $z_i$  the charge,  $D_i^{o/w}$  is the diffusion constant in the water, and all other letters have their usual meaning.

The mass transport of a specific ion  $i$  in between the layers and thus through interfaces was modelled using the Butler-Volmer-type relations:

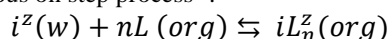
$$i^z(w) \xrightleftharpoons[k_b]{k_f} i^z(org)$$
$$k_f = k_0 \exp \left[ -\frac{\alpha z F (\varphi - \varphi^0)}{RT} \right]$$
$$k_b = k_0 \exp \left[ \frac{(1 - \alpha) z F (\varphi - \varphi^0)}{RT} \right]$$

Where  $\varphi$  is the potential drop over the interface (transfer potential);  $\varphi^0$  is the standard transfer potential<sup>a</sup> at  $k_f = k_b$ ;  $\alpha$  is the transfer coefficient;  $k_0$  is the standard heterogeneous rate constant;  $k_f/k_b$  forward/backward heterogeneous rate constant and the other letters have their usual meaning.

---

<sup>a</sup> Note that standard transfer potentials are used instead of formal transfer potentials. Consequently, it is implicitly assumed that the activity coefficients within the organic phase and the aqueous phase are unity.

In case of a facilitated transfer of a specific ion by an ionophore and of stable ion-ionophore complexes, the ion transfer be considered as a heterogeneous on step process <sup>8</sup>:



Where L is the ionophore and n the complex stoichiometry.

The energy required to transfer the ion into the membrane is decreased by the complex formation constant ( $\beta$ ) of the ionophore. According to the thermodynamic cycle approximation the formal potential  $\varphi^0$  can be described by <sup>9</sup>:

$$\varphi^0 = \varphi_i^0 + \frac{RT}{zF} \ln \beta_n L^n$$

Where  $\beta_n$  is the complex formation constant within the ISM and  $\varphi_i^0$  is the simple ion transfer potential and  $L^n$  is the concentration of the free ionophore within the membrane

The NPP equations approximate the ions by point charges with an infinite small size not accounting for any concentration dependent activity changes or adsorption effects at the ISM-water interface. Thus the NPP equation model the diffuse Gouy-Chapman layer. However, the stern layer, which greatly depends on the size of the ions, on adsorption process, interaction of present ions and other complex processes, cannot be modelled. For that reason, to calculate the potential drop over the interface ( $\varphi$ ) the stern layer is approximated by a capacity; i.e. the potential is obtained by multiplying the electric field at the phase boundary by the distance in between the interfaces. The dielectric constant of the capacity was assumed to be the arithmetic average of the dielectric constant of the water and the NPOE.

Similar to ref. <sup>2</sup> the method of lines was used to discretize the differential equations. This method is illustrated in figure S1. The program was written in Octave, which is an open source pendant of matlab. The equations were integrated using the Octave Isode solver. Alternatively, it is also possible to use the odesx solver of the odepkg (wrapper of the fortran seulex solver). The calculations were carried out on a 64 bit - windows 8 system taking full advantage of the new 64 bit Octave build.

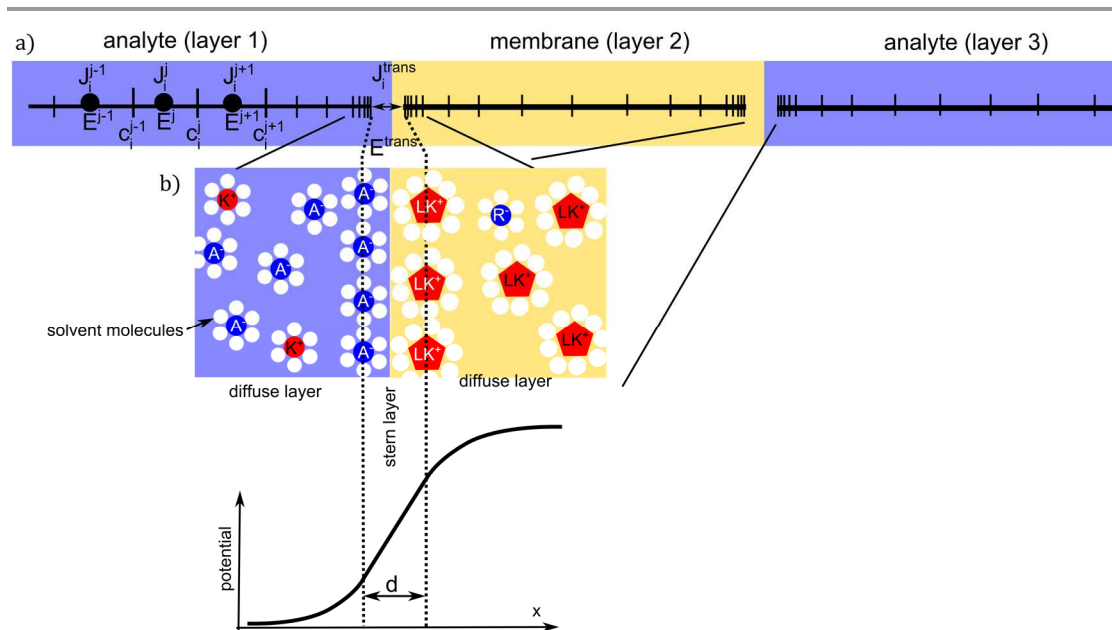


Figure S1: a) Illustration of the numerical calculations and the discretisation used. The spacing of the grid where the concentration was calculated was chosen to be smaller closer to the interfaces. The flux and the electric field are calculated at intermediate points lying half way between the concentration points. The transfer rates/transfer potentials were calculated by assuming a stern layer at the interface with a discrete distance  $d$  (b). The  $LK^+$  complex is illustrated by a red pentagon; A corresponds to anions present in the analyte, R to background anions in the membrane and  $K^+$  to potassium ions in the analyte,

### Parameters used for the numerical calculations

The parameters were taken from literature (see table 1 and table 2), if they were available. Due to very complex experimental setup and assumptions which have to be made (e.g. diffusion constants), there is a large discrepancy of the experimental values in literature. To qualitatively model the sensor response, this is obviously not a hindrance as the simulated response curves are in good agreement with the experimental results.

Most of the simple ion transfer potentials measured in literature are measured at a NPOE/W micro interface. As the PVC does not seem to influence the transfer potentials significantly (just  $\sim 20$  mV)<sup>10</sup>, the values obtained at NPOE/W interfaces seem to be justified.

In case of highly hydrophilic ions ( $\text{Ca}^{2+}$ ,  $\text{SO}_4^{2-}$ ) no experimentally obtained values of the formal transfer potential are available yet. Typically the ion transfer potentials are measured by CV measurements which require a background electrolyte in the organic phase. This background electrolyte within the membrane typically gets extracted before these lipophilic ions are extracted into the membrane. For that reason the transfer potentials were assumed to be larger than the transfer potentials of the background electrolyte within the membrane used.

Table 1: Parameters used to numerical compute the NPP equations.

Ion	$D_o$ [ $\text{m}^2/\text{s}$ ]	$D_w$ [ $\text{m}^2/\text{s}$ ] <sup>f</sup>	$\varphi_i^0$ [mV]	Log $\beta$
$\text{K}^+$	$1.3 \cdot 10^{-11,\text{a}}$	$1.96 \cdot 10^{-9}$	<b>440<sup>g</sup></b>	<b>11.63<sup>l</sup></b>
$\text{IL}^+$	<b><math>3.01 \cdot 10^{-12,\text{b}}</math></b>	n.a.	n.a.	<b>11.63<sup>l</sup></b>
$\text{Cl}^-$	$1.3 \cdot 10^{-11,\text{a}}$	$2.03 \cdot 10^{-9}$	<b>-521<sup>h</sup></b>	<b>0</b>
$\text{Na}^+$	$8.8 \cdot 10^{-12,\text{a}}$	$1.33 \cdot 10^{-9}$	<b>518<sup>g</sup></b>	$7.63^{\text{m}}$
$\text{TCIPB}^-$	$1.1 \cdot 10^{-12,\text{c}}$	$1.66 \cdot 10^{-10}$	<b>-335<sup>i</sup></b>	<b>0</b>
$\text{Ca}^{2+}$	$5 \cdot 10^{-11,\text{a}}$	$7.54 \cdot 10^{-10}$	$350^{\text{j}}$	0
$\text{TDA}^+$	$0.6 \cdot 10^{-12,\text{d}}$	$0.9 \cdot 10^{-11}$	$-500^{\text{j}}$	0
Ionophore I	<b><math>1.9 \cdot 10^{-12,\text{b}}</math></b>	n.a.	n.a.	n.a.
$\text{SO}_4^{2-}$	$7 \cdot 10^{-11,\text{a}}$	$10.7 \cdot 10^{-9}$	$-300^{\text{k}}$	0
$\text{TFPB}^-$	$1.1 \cdot 10^{-12,\text{e}}$	$1.66 \cdot 10^{-10}$	n.a.	0

a) The diffusion coefficients were calculated using the estimated ratio of  $D_o/D_w = 6.6 \times 10^{-3}$  as proposed in ref. <sup>12</sup>; b) taken from ref <sup>13</sup>; c) assumed to be equal to the diffusion coefficient of TFPB<sup>-</sup>, which has a very similar size and structure; d) The diffusion coefficient of TDA was assumed to be twice as big as TFPB<sup>-</sup> which is  $\sim 2$  times smaller; e) taken from ref. <sup>14</sup>; f) taken from ref. <sup>15</sup> and ref. <sup>16</sup>; g) taken from <sup>17</sup>; h) taken from <sup>18</sup>; i) taken from ref <sup>16</sup>; j) taken from ref <sup>18</sup>. The value of TDA was estimated from the graphs available in <sup>18</sup>; k) The value was estimated from the data available in ref. <sup>19</sup> in a nitrobenzene/water interface as proposed in ref <sup>18</sup> and <sup>16</sup>; l) taken from <sup>20</sup>; m) assumed.

Table 2: Parameters used to numerical compute the NPP equations.

Parameter	Value
$\epsilon_{\text{water}}$	80
$\epsilon_{\text{membrane}}$	$40^{\text{a}}$
membrane thickness	$150 \mu\text{m}$
water layer thickness	$400 \mu\text{m}$
interface distance (d)	$2 \text{ nm}^{\text{d}}$
$k_0$	$9 \cdot 10^{-3} \text{ cm/s}^{\text{c}}$
$\alpha$	$0.48^{\text{c}}$

a) taken from <sup>21</sup>; c) the standard rate constants and the transfer coefficients were assumed to be equal for all transferring ions. The value was taken from ref. <sup>8</sup>; d) assumed.

## S2 Dynamic response at small pulse times

The actual response at small pulse time before depletion effects occur is not intuitive: The reactions at the interface are fast and instantaneous establishing a near-nernstian phase boundary potential, even under dynamic mass transport conditions (as long as no concentration polarization occurs)<sup>1,22</sup>. This near-nernstian phase boundary potential is not equal to the one measured under zero current conditions because the phase boundary activities change. The current induced activity change greatly depends on the diffusion constant within the respective phase. As long as there are sufficient target ions or free ionophores available, the phase boundary potential, remains near Nernstian.<sup>53,132</sup> If the concentration of the target ion is smaller than a critical concentration, the ion is depleted in the vicinity of the membrane at a certain transition time and a potential jump exceeding the Nernstian response is observed.

Figure S3 a and b show the corrected experimental and numerically calculated response curves at small pulse times of  $\text{ISE}_{\text{IN}}$  and  $\text{ISE}_{\text{OUT}}$  respectively. The curves were corrected for the initial equilibrium potential (which cancels out in the final response curve) ,measured before the current pulse was applied. The corrected potentials recorded at fixed times  $t_1$  (1s) and  $t_2$  (2s) are shown in c / d. Generally, the corrected potentials measured at time  $t_1$  are smaller than the ones measured at  $t_2$ .

In case of  $ISE_{IN}$  and at large target ion concentrations ( $> 1$  mM), the potential does not depend noticeably on the concentration of the target ions within the analyte (see figure S2 a,c). However, it increases with time. This increase can be attributed to a magnitudes smaller ion diffusion constant in the membrane than in the aqueous phase: The phase boundary concentrations within the membrane are gradually increased on the front and decreased on the backside. Whereas, the phase boundary concentration within the analyte remain almost unchanged. Consequently, the constant current induces a concentration independent response. At a concentration of 1 mM the target ion is depleted and the response depends on the ion concentration within the analyte.

Similar to  $ISE_{IN}$ , the response of  $ISE_{OUT}$  does not depend on the sample composition at high target ion concentrations ( $> 1$  mM), as long as no backside depletion occurs (see figure S2 b,d). At a concentration of 0.1 mM the phase boundary concentration of the analyte is slightly changed giving rise to a response drift of  $\sim 20$  mV which is a negligible contribution to the total sensor response. Note that this shift does not degrade the sensing signal as it depends selectively on the concentration of the target ion. However, if the signal would be measured at  $t_2$  the response would strongly depend on the background anion present in the analyte (see figure S2 d).

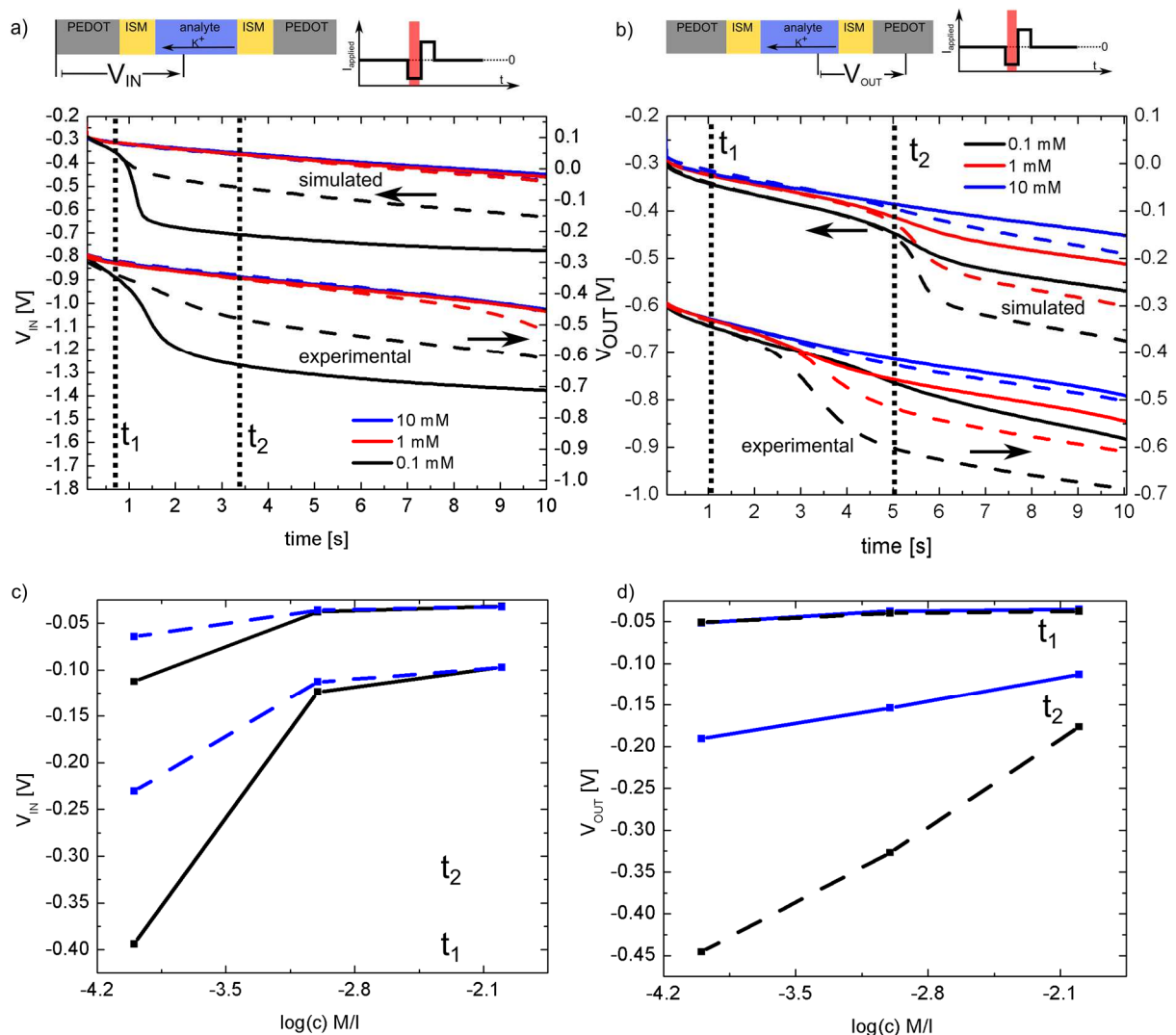


Figure S2: Experimentally and numerically calculated corrected response curves at small pulse times of  $ISE_{IN}$  (a) and  $ISE_{OUT}$  (b) recorded in a  $CaCl_2$  (solid lines) and  $Na_2SO_4$  (dashed lines) background at concentrations of 0.1 mM, 1 mM and 10 mM. The response curves were obtained by subtracting the equilibrium potential measured under zero current conditions at the end of the regeneration pulse. The corrected response recorded at  $t_1$  (1s) and  $t_2$  (2s) are shown in c) ( $ISE_{IN}$ ) and d) ( $ISE_{OUT}$ ).

### S3 Numerically calculated concentration profiles

The response curves and the corresponding concentration profiles of the ions at  $ISE_{IN}$  and  $ISE_{OUT}$  are shown in figure S3 and S4 respectively. The response curves which are corrected for the initial equilibrium potential are shown in the insets.

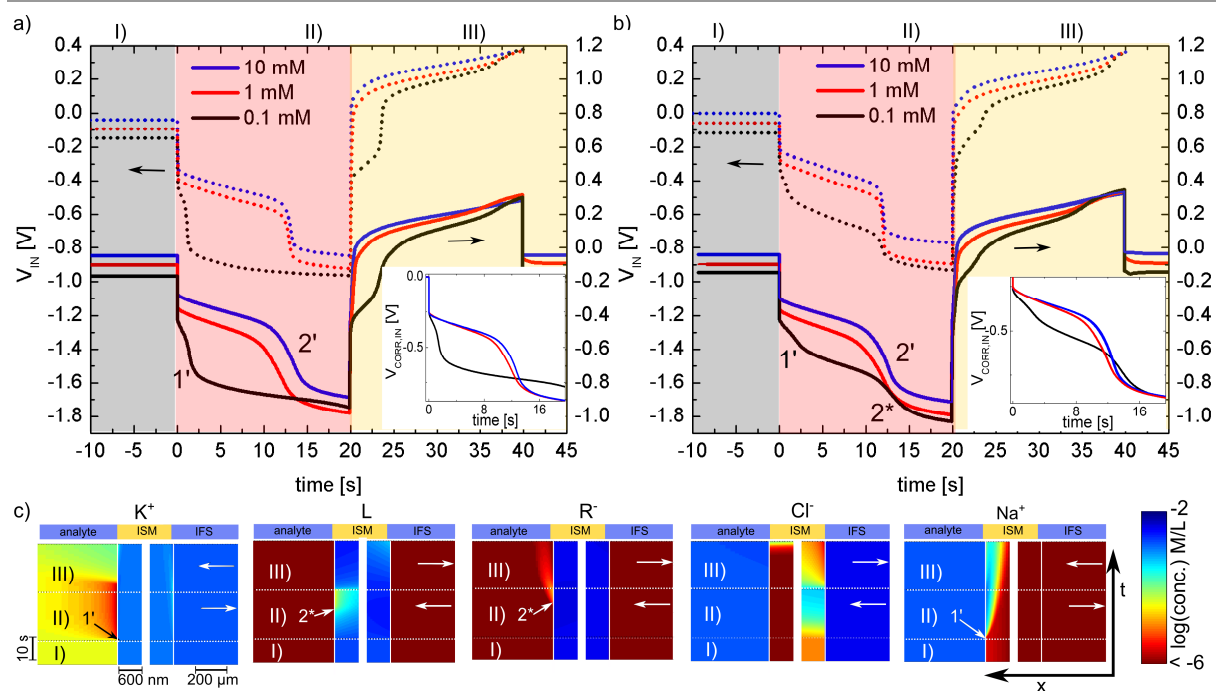


Figure S3: Measured (solid) and numerically calculated (dotted) response of  $ISE_{IN}$  during a measurement cycle at concentrations of 0.1 mM, 1 mM and 10 mM KCl in a 10 mM  $CaCl_2$  background (a) and a 10 mM NaCl background (b). The insets show the corrected potentials ( $V_{IN}(t) - V_{IN}(t = -5 \text{ s})$ ). The characteristic transition times are marked with numbers (for details see text). The applied current density was  $0.4 \mu A/mm^2$ . c) Calculated concentration profiles at the interfaces of the relevant ions during a measurement cycle at a concentration of 0.1 mM  $K^+$  in a NaCl background. The time and location where characteristic transitions occur are marked with numbers (for details see text). For better visibility, the x-axis are scaled differently for each ion in the membrane as well as in the aqueous solutions.

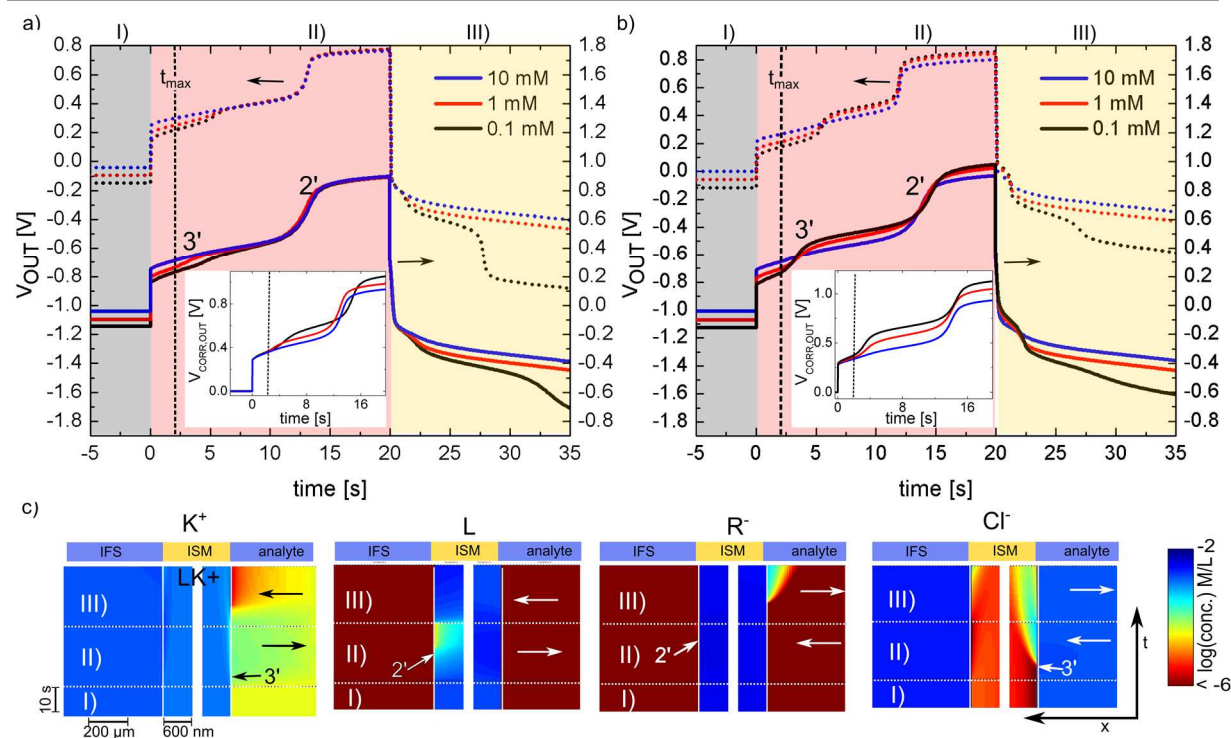


Figure 1: Measured (solid) and numerically calculated (dotted) response of  $ISE_{OUT}$  during a measurement cycle at concentrations of 0.1 mM, 1 mM and 10 mM KCl in a 10 mM  $CaCl_2$  background (a) and a 10 mM  $Na_2SO_4$  background (b). The insets show the corrected potentials ( $V_{CORR,OUT} = V_{OUT}(t) - V_{OUT}(t = -5 \text{ s})$ ). The characteristic transition times are marked with numbers (for details see text). The applied current density was  $0.4 \mu A/mm^2$ . The maximum applicable pulse time ( $t_{max} \sim 2 \text{ s}$ ) is marked by a vertical line. c) Calculated concentration profiles at the interfaces of the relevant ions during a measurement cycle at a concentration of 0.1 mM in a  $CaCl_2$  background. The times and locations where characteristic transition times occur are marked with numbers (for details see text). For better visibility, the x-axis are scaled differently for each ion in the membrane as well as in the aqueous solutions.

## S4 Stability and conditioning investigations

Figure S3 shows the response curves of SC-ISE<sub>IN</sub> and SC-ISE<sub>OUT</sub> recorded in a 0.1 mM KCl solution. The first and second response curves exhibit significant drifts. After 15 measurement cycles the response curves reach a steady state and there are only small shifts in the thereafter following measurements. If the ISE is left idle for a day a significant change from measurement to measurement is observed in the beginning. Same as before, after 15 measurements the response curves reach a steady state and are almost identical to the ones measured on the first day. Consequently 15 conditioning measurements have to be carried out prior to measurement. The response curves are generally more reproducible at the beginning of the pulse and even after three months and 120 measurements, the response curve remains almost unchanged. Figure S3 also demonstrates the advantage of 2 ISEs operated in series. In equilibrium, before the measurement pulse is started, the potentials of the ISEs exhibited a drift of 130 mV after 3 months with respect to an Ag/AgCl reference electrode. If just one ISE would have been used this would have resulted in a potential shift of ~130 mV (see figure S3b). As both ISEs are identical they both exhibit approximately the same potential drift. For that reason the net potential between the ISEs is not changed. Thus the sensor response is not influenced by this drift.

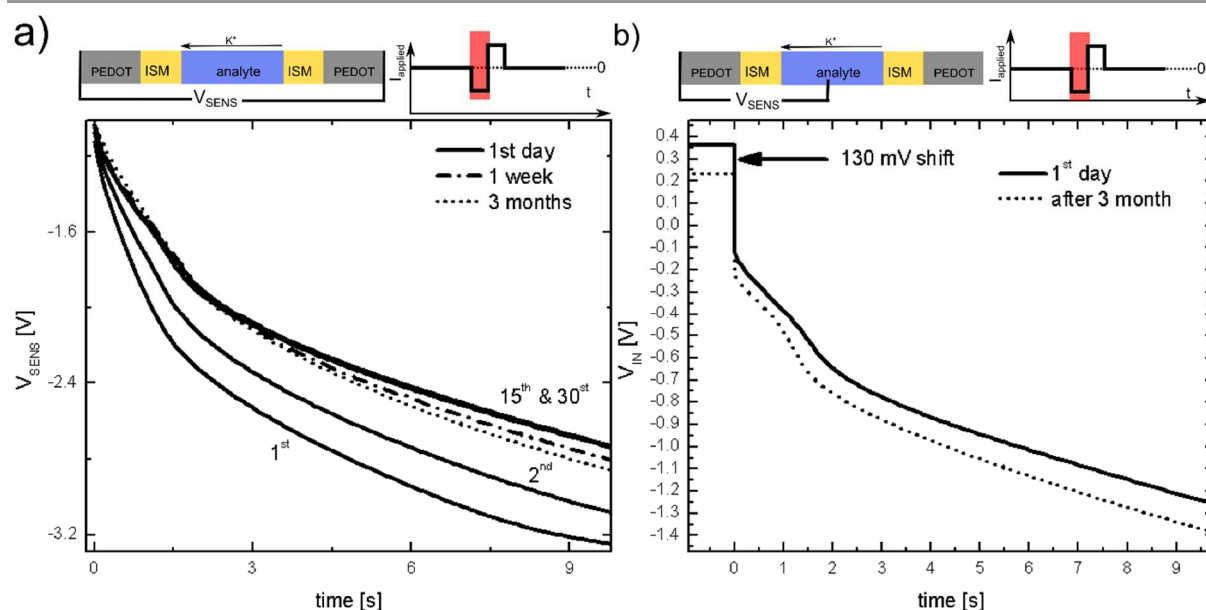


Figure S3: Sensor response (a) and response of ISE<sub>IN</sub> only (b) during a current pulse ( $\sim 0.6 \mu\text{A}/\text{mm}^2$  ISE<sub>IN</sub> and  $0.4 \mu\text{A}/\text{mm}^2$  ISE<sub>OUT</sub>) in a  $10^{-4}$  M K<sup>+</sup> solution after 15 and 30 measurements on the first day (solid lines) and the thereafter following measurement at the second day (dash-dot lines) and after 3 months (dotted lines). The illustration on the top shows the measurement setup and the time span which is shown in the graph (red area)

## Notes and references

<sup>a</sup> NanoTecCenter Weiz Forschungsgesellschaft m.b.H., Franz-Pichler-Straße 32, A-8160 Weiz, Austria.

<sup>b</sup> Institute of Solid State Physics, Graz University of Technology, Petersgasse 16, A-8010 Graz, Austria

<sup>1</sup> A. Shvarev and E. Bakker, *Anal. Chem.* **75**, 4541 (2003).

<sup>2</sup> B. Gryszakowski, A. Lewenstam, and M. Danielewski, *Diffus. Fundam.* **8**, 1 (2008).

<sup>3</sup> T. Sokalski, P. Lingenfelter, and A. Lewenstam, *J. Phys. Chem. B* **107**, 2443 (2003).

<sup>4</sup> J.M. Zook, S. Bodor, R.E. Gyurcsányi, and E. Lindner, *J. Electroanal. Chem.* **638**, 254 (2010).

<sup>5</sup> J.M. Zook, R.P. Buck, R.E. Gyurcsányi, and E. Lindner, *Electroanalysis* **20**, 259 (2008).

<sup>6</sup> E. Bakker and a. J. Meir, *SIAM Rev.* **45**, 327 (2003).

<sup>7</sup> J.J. Jasielec, R. Filipek, K. Szyszkiewicz, J. Fausek, M. Danielewski, and a. Lewenstam, *Comput. Mater. Sci.* **63**, 75 (2012).

- <sup>8</sup> R. Ishimatsu, A. Izadyar, B. Kabagambe, Y. Kim, J. Kim, and S. Amemiya, *J. Am. Chem. Soc.* **133**, 16300 (2011).
- <sup>9</sup> R. Ishimatsu, A. Izadyar, B. Kabagambe, Y. Kim, J. Kim, and S. Amemiya, *J. Am. Chem. Soc.* **133**, 16300 (2011).
- <sup>10</sup> J. Langmaier, K. Stejskalová, and Z. Samec, *J. Electroanal. Chem.* **496**, 143 (2001).
- <sup>11</sup> O.L. Francois, P. Sun, and M. V Mirkin, *J. Am. Chem. Soc.* **1128**, 15019 (2006).
- <sup>12</sup> T. Osakai, Y. Sato, M. Imoto, and T. Sakaki, *J. Electroanal. Chem.* **668**, 107 (2012).
- <sup>13</sup> J.M. Zook, S. Bodor, E. Lindner, K. Tóth, and R.E. Gyurcsányi, *Electroanalysis* **21**, 1923 (2009).
- <sup>14</sup> S. Bodor, J.M. Zook, E. Lindner, K. Tóth, and R.E. Gyurcsányi, *J. Solid State Electrochem.* **13**, 171 (2008).
- <sup>15</sup> Y.-H. Li and S. Gregory, *Geochim. Cosmochim. Acta* **38**, 703 (1974).
- <sup>16</sup> M. Imoto, T. Sakaki, and T. Osakai, *Anal. Chem.* **85**, 4753 (2013).
- <sup>17</sup> H.J. Lee, C. Beriet, and H.H. Girault, *J. Electroanal. Chem.* **453**, 211 (1998).
- <sup>18</sup> S. Wilke and T. Zerihun, *J. Electroanal. Chem.* **515**, 52 (2001).
- <sup>19</sup> T. Osakai, T. Kakutani, Y. Nishiwaki, and M. Senda, *Anal. Sci.* **3**, 499 (1987).
- <sup>20</sup> Y. Qin, Y. Mi, and E. Bakker, *Anal. Chim. Acta* **421**, 207 (2000).
- <sup>21</sup> E. Lindner, E. Graf, Z. Niegreis, K. Toth, E. Pungor, and R.P. Buck, *Anal. Chem.* **60**, 295 (1988).
- <sup>22</sup> E. Bakker, P. Bühlmann, and E. Pretsch, *Chem. Rev.* **97**, 3083 (1997).